Fabrication and Characterization of PLA Scaffolds for Bone Tissue Engineering

Yudan Whulanza, Jos Istiyanto, Taufiq Ramadhan

Department of Mechanical Engineering, Faculty of Engineering, Kampus UI Depok, Indonesia 16424

Abstract: In order to regenerate damaged tissue in human, a method termed as tissue engineering uses scaffolds as cell pathway to reconnect with original tissue was introduced. Recently, additive manufacturing technique allows production of 3D scaffold construct where biomaterial and cells can be directly located in predetermined spatial arrangement. In this research, a commercial fused deposition modeling system, Reprap Mendel™, is employed so that it enables us to realize microenvironment composed of biodegradable material i.e. polylactic acid. Furthermore, simple geometries are proposed and later mechanically characterized in term of stiffness and porosity. This research focuses on the design and realization of 3D scaffold with various sizes and geometries. Variations of these parameters will result in scaffolds with porosity correlated to the value of the modulus of elasticity (E). The measurement shows that our scaffolds have a porosity ranging from 24% -77% with a modulus of elasticity ranging from 1.6 to 4.5 MPa.
Keywords: tissue engineering, scaffolds fused deposition modeling, polylactic acid.

1. Introduction

It is noted that bone clinical problems are caused by several factors such as abnormality, accidents and osteoporosis. In case of osteoporosis, the Federal Drug Association reported that there are 1.5 million casualties every year with female as majority [1]. Additionally, the report also mentioned that there was significant relationship between bone densities with age. In a denser bone, higher modulus elasticity was indicated. It was also found that young generation has elastic modulus of around 1,390 MPa. Moreover, a decrease of elastic modulus is indicated for middle and older generation namely 1,290 and 940 MPa respectively [2].

Bone tissues is known to have a limitation in self-recovery, thus an alternative therapeutic is needed. A common method that already employed is bone grafting. However, this method has disadvantages such as infection and contagion during grafting process. Therefore, tissue engineering approach is introduced in the end year of 90s. Tissue engineering grows new tissues or organs from original cell ex-vitro by means of tissue scaffolds. The scaffold serves as medium for cells to be propagated and implanted as the maturity of corresponded cells is achieved. Principally, scaffolds emulate extracellular matrix (ECM) which consisted of protein fibers as cells regeneration media. ECM has mechanical integrity as supporting structure of cells to immobilize, differentiate, motility and cell crosstalk [3-5]. Therefore, a scaffold must fulfill several criteria such as biocompatible, biodegradable, porous and geometrically alike but also has sufficient mechanical properties.

There have been several methods employed in order to match the geometrical and material consideration of an ideal scaffold. A micro computed tomography was utilized to resemble an original bone tissue. This approach remarkably mimics a bone scaffold in term of volume, porosity and trabecular thickness. However, this scaffold was impossible to implant since the structure has inability to grow [6]. It is indicated that a "living structure" is much more needed. Therefore, researches in field of fabricating and material developing are flourished during the past ten years.

This paper investigates realization of scaffolds using a technique so called fused deposition modeling. FDM deposited a polymer filament layer by layer based on pre-designed structure. This technique has been introduced by Hutmacher to create porous scaffold with pore size of around 0.25 mm^2 [7]. He reported the porosity achieved and degradability of the material namely polyglycolide (PGA) and polylactides (PLLA, PDLA). Additionally, Mulder highlighted the development of additive manufacturing technology in realizing porous structure [8]. More recently, porous bioactive glass was also realized to explore the interaction of host cell [9]. However, the relationship between realized porous structure and mechanical property was not yet explained among those reports. In this paper, various geometries and pore sizes were realized. Later, the compressive test was performed to relate the

*Corresponding author E-mail: yudan@eng.ui.ac.id

porosity that established from those structures. Ultimately, finite element model was also setup to explain the mechanical behavior under a static load.

2. Material and Method

2.1 *Porous Scaffold Realization*
A Reprap Mendel^{TM} is utilized to realize scaffold specimen with a dimension of 12.5x12.5x12.5 cm^3, 15x15x15 cm^3 and 18x18x18 cm^3. Corresponded to those dimensions, pore sizes that will be realized are 0.25 mm^2, 0.36mm^2 and 0.52 mm^2. Moreover, several porous scaffolds were also realized such as quadratic, cross and combined quadratic-cross (figure 1).
The diameter nozzle used was 0.5 mm with diameter of polylactide filament equal to 1.75 mm. the platform bed as x-y plane was set at 10, 30 and 50 mm/s. Later on, extrusion parameter was governed at 6 mg/s. Nozzle temperature was set at 180^oC as polylactide melting point, whereas bed temperature was set at 60^oC.

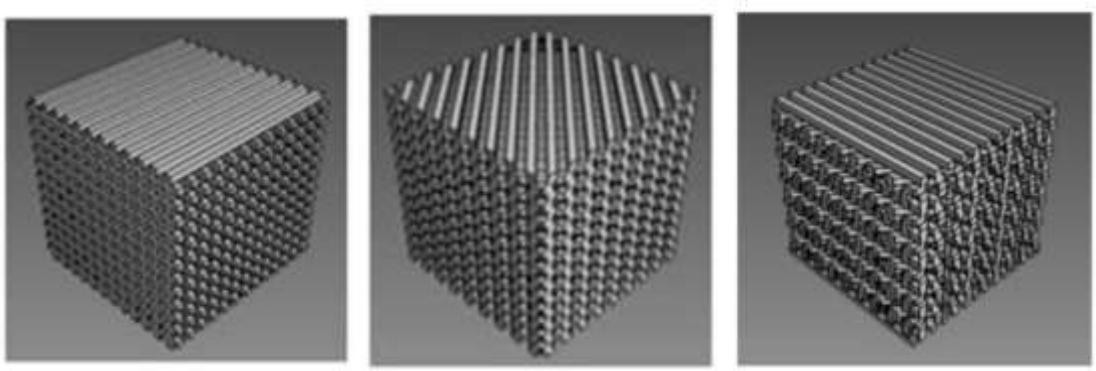

Figure 1. *Scaffolds with Various Designed Geometries*

2.2 *Geometric Measurement*
Optical microscopy was used to investigate the structure and evaluate the microstructure of realised 3D scaffolds. Olympus AX70 optical microscope equipped with Olympus C-5060 Camera and image processing software was utilized.

2.3 *Compressive testing*
Compressive modulus was measured using Ultimate Testing Machine Gotech-AI-7000. Deformation rate was set at 0.2 mm/minute until 50% of its original height. Four samples were tested for each measurement and performed as mean ± standard deviation.

2.4 *Porosity Measurement*
Porosity scaffolds was measured using water evaporation method. The sample was immersed in volumetric glass thus filling void space inside the sample. Later on, gravimetric test was performed to measure the water volume that trapped inside specimen. It is assumed that water was perfectly removed during emptying water inside the specimen. Later, equation 1 and 2 were determined to calculate the porosity of samples.

$$Vpores = \frac{(m\,wet - m\,dry)}{\rho\,air} \quad (1)$$

$$Porosity = \frac{\text{V pori}}{\text{V total}} \text{ x } 100\% \quad (2)$$

V pores = *Porous volume (mm^3)*
m_{wet} = *Sample mass in wet condition*
m_{dry} = *Sample mass in dry condition*
V_{total} = *Bulk volume*

2.4 *Numerical Simulation*
Porosity scaffolds was measured using water evaporation method. The sample was immersed in

volumetric glass thus filling void space inside the sample. Later on, gravimetric test was performed to measure the water volume that trapped inside specimen. It is assumed that water was perfectly removed during emptying water inside the specimen. Later, equation 1 and 2 were determined to calculate the porosity of samples

3. Result and Discussion

3.1 *Geometrical Characterization*

Principally, there are two parameters that need to be optimized which are speed of x-y plate and extrusion parameter. Figure 2 depicts the line width that achieved from parameter arrangement. Figure 2a reveals that there is a significant dependency between plate speed and realized line width (anova test p-value 0.04). The higher x-y plate speed, the narrower line width resulted. It can be inferred that polymer filament acts as viscoelastic material. The higher speed plate resulted in higher viscosity of filament.

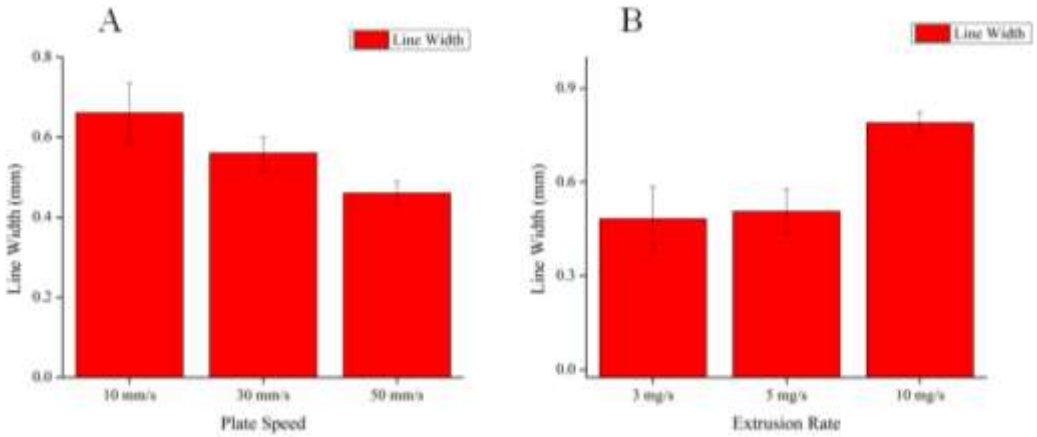

Figure 2. Realized Line Width at Various Parameters

Figure 2b depicts the resulted line width at various extrusion rates. It shows that extrusion rate of 3-5 mg/s has no significant

change in line dimension. Moreover, figure 3 summaries the result of two parameters in realizing line scaffolds. A "good" attribute was indicated that the line has a standard deviation lower than 10% and width of less than 0.5 mm. Hence, this arrangement is then used to fabricate scaffold specimens.

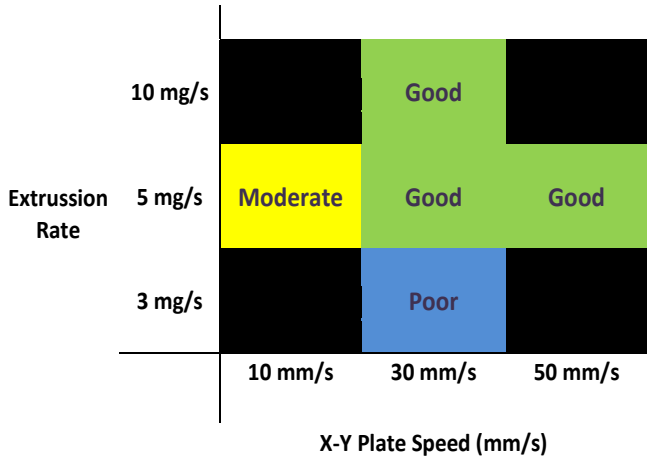

Figure 3. Working Diagram of Reprap^{TM} in Realizing Line Scaffolds

3.2 *Scaffold Characterization*

3.2.1 *Scaffold with Various Pore Size*

Figure 4 depicts the realized scaffold with quadratic geometry. The parameter chosen was 30 mm/s with extrusion rate of 5 mg/s. It can be noted that the line width is the range of 0.5 mm. Moreover, it also can be indicated that the pore size is about 0.9x0.9 mm^2. Figure 4b shows the design and the realized dimension of pore. Pore size of 0.25 mm^2 and 0.36mm^2 has a relatively small mismatch between design and realized. On the other hand, pore size of 0.52 mm^2 has relatively high standard deviation.

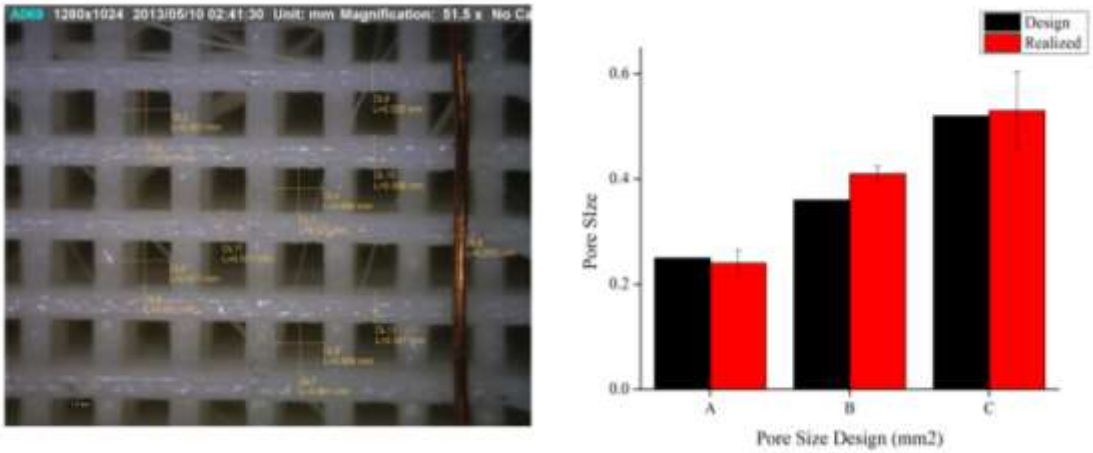

Figure 4. Realized Scaffolds and Pore Size Design

Figure 5 shows the result of porosity and elastic modulus measurement. A solid cube was also realized as reference for zero porosity. However, the porosity measurement shows a value of 1% for the solid specimen. It can be concluded that a small amount of water was remain in the specimen after drying process. However, a relative low value indicates that we can assume that it can be neglected.

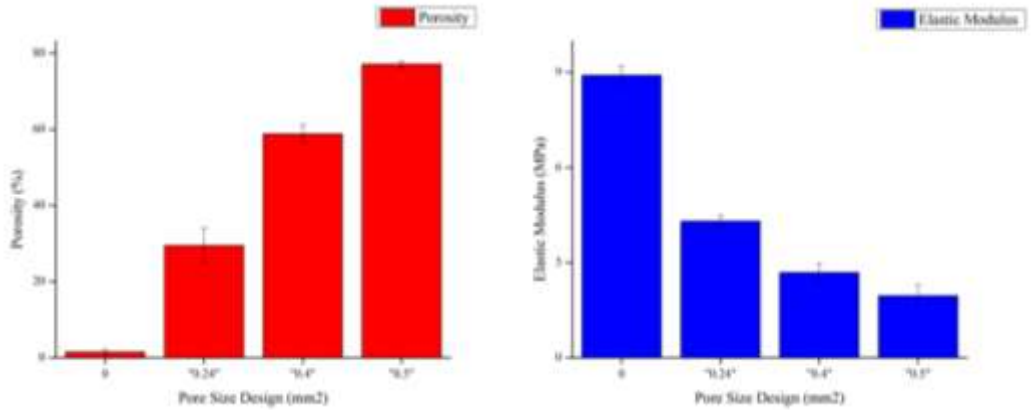

Figure 5. Results of Porosity and Elastic Modulus Measurement for Various Pore Size

A compressive test was employed for PLA scaffold specimens. Later, elastic modulus was calculated from its gradient in linear elastic deformation. Figure 5b indicates that the bigger porous, the lower elastic modulus resulted. Thus, more ductile scaffolds of 3D feature are formed. Here, elastic moduli are found in the range of 4.3±0.18; 2.7±0.28 and 2.0±0.34 MPa for pore size of 0.24; 0.4 and 0.5 mm2 respectively.

Figure 6 shows the result of compression until 10% of its original longitudinal direction. It can be reported that no elongation break was evident until 300% of deformation for all pore size design. This behavior is indicated a plastic deformation region was found trough out this strain area. Furthermore, it can be concluded that the yield strength of pore size 0.24 mm^2 is the highest. Later, it is followed by 0.4 and 0.5 mm^2 consistently. Intuitively, this finding shows that the more compact of structure, the stronger structure is resulted.

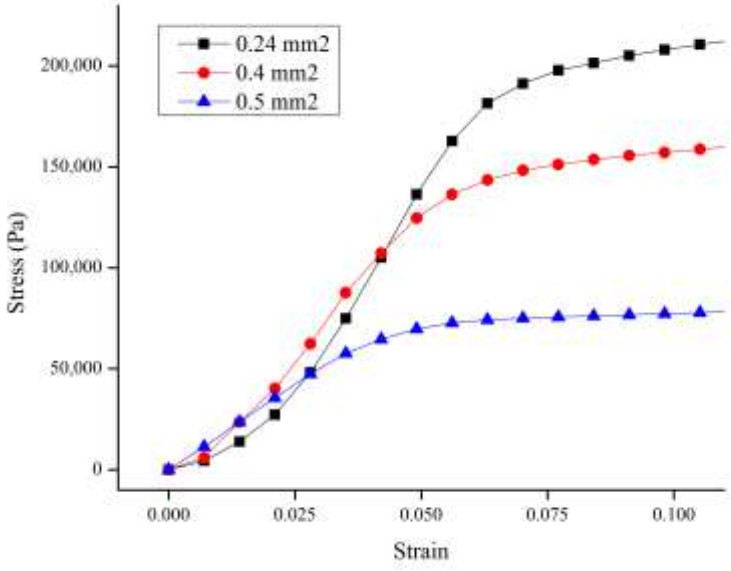

Figure 6. Typical Stress Strain Curve Resulted from Scaffolds with Various Pore Size

3.2.2 *Scaffold with Various Geometries*

Figure 7 depicts realized scaffolds with various geometries which are cross and combine between quadratic and cross. Quadratic geometry was already shown in figure 4 above. Same as figure 4 above, it is also shown a wire with diameter of 0.25 mm as reference dimension. Here, we aimed to investigate the correlation between geometry and its resulted mechanical properties. All pore size was designed at 0.4 mm^2.

Figure 7. Realized Scaffolds with (A) Cross Geometry and (B) Combined Cross-Quadratic Geometry

Figure 8 indicates that porosity formed from all geometry is alike. It is in the range of 60% with similar standard deviation. Anova test reveals no significant difference between porosity with various geometries. On the other hand, elastic modulus of combine geometry shows a significant difference

with quadratic geometry. However, the range of elastic moduli resulted are in the range of 2.5 MPa. This finding concludes that geometries that already investigated do not modify the mechanical property significantly.

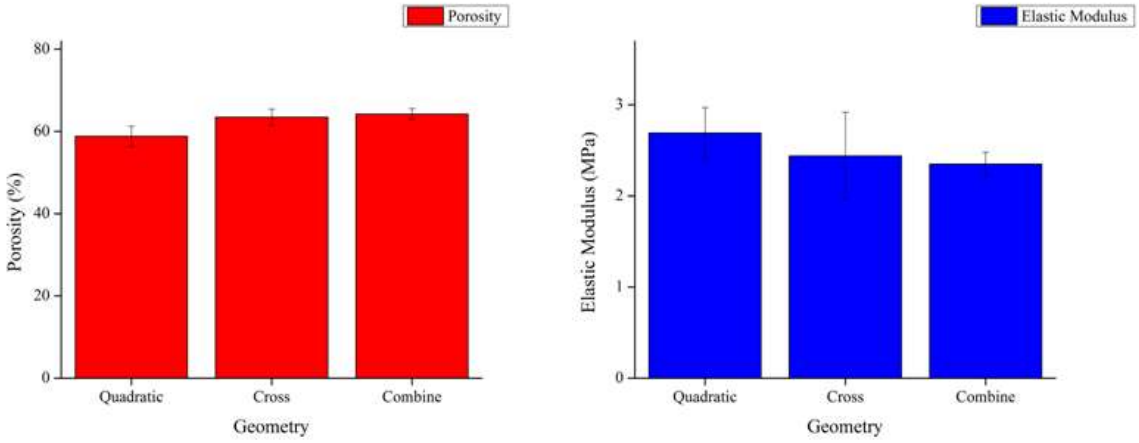

Figure 8. Results of Porosity and Elastic Modulus Measurement for Various Geometries

Figure 9 depicts the result of compressive test in various specimens. It can be highlighted that the quadratic geometry has highest strength compare to others. On the other hand, the cross geometry has lowest strength. Thus in combination between the two, an intermediate strength is resulted. Moreover, no elongation break was indicated during the compressive test for all geometries.

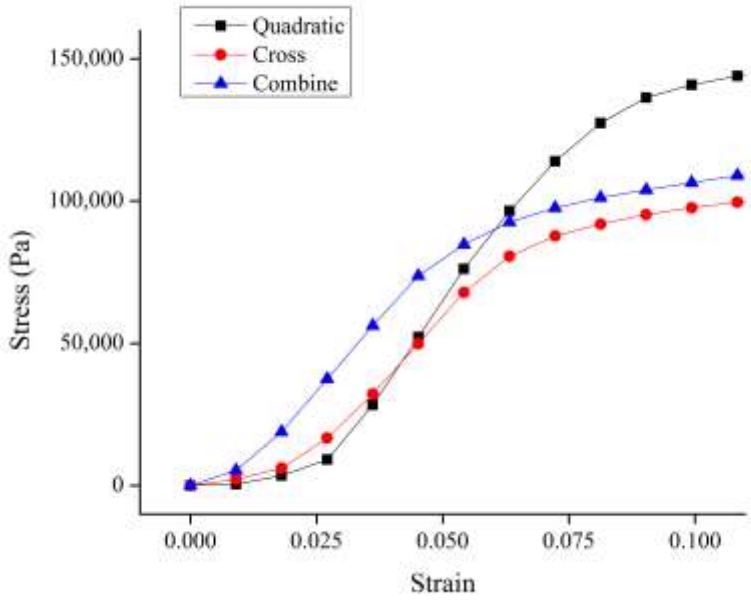

Figure 9. Typical Stress Strain Curve Resulted from Scaffolds with Various Geometry

3.3 *Numerical Simulation*

Ultimately, a finite element simulation is conducted to study the scaffold in static loading scenario. ANSYS^{TM} environment was used to simulate the compressive loading. Simulation parameter such as

elastic modulus, density and loading were drawn from experimental, whereas the Poisson ratio was set at 0.36 as literature review. A force of 45 N was introduced in the simulation as in compressive test.

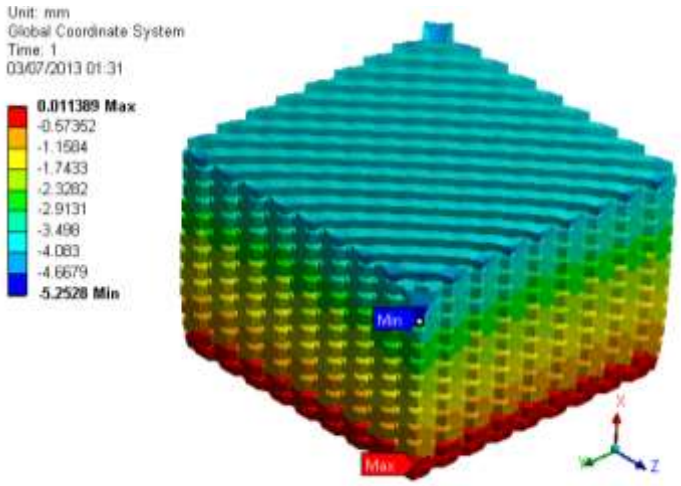

Figure 10. Static Load Simulation of Scaffold with Cross Geometry

Figure 10 depicts the deflection resulted from the loading simulation. The simulation indicates that quadratic geometry has the lowest deflection. This result agrees with our experimental above that quadratic has the highest stiffness and strength. However, a mismatch of 10-305 was found between simulation and experimental result. An experimental Poisson value might be needed to get more accurate result. However, the simulation shows a plausible explanation by resulting similar trend in geometry variation.

4. Conclusions

The realization of scaffolds with adjusted pore size was successfully experimented. We also optimized the working parameter for our FDM equipment. Moreover, the relationship between pore size design and mechanical porosity is also studied here. Ultimately, a FEM model of the scaffold is realized which can be improved in the next experiment.

5. References

[1] U.s. Public Health Service; Bone Health and Osteoporosis - A Report of the Surgeon General, Rockville, MD; 2004.
[2] Ding M. et al; Mechanical Properties of the Normal Human Tibial Cartilage-Bone Complex in Relation to Age;1997.
[3] Mandal, B. B. and Kundu, S. C. Non-bioengineered high strength three-dimensional gland fibroin scaffolds from tropical non-mulberry silkworm for potential tissue engineering applications. Macromolecular Bioscience. 2008; 8; 807-818.
[4] Mandal, B. B. & Kundu, S. C.. Cell proliferation and migration in silk fibroin 3D scaffolds. Biomaterials. 2009; 30; 2956-2965.
[5] Mandal, B. B. and Kundu, S. C. Osteogenic and adipogenic differentiation of rat bone marrow cells on non-mulberry and mulberry silk gland fibroin 3D scaffolds. Biomaterials. 2009; 30; 5019–5030.
[6] Liebschner M.A.K and Wettergen MA. Optimization of Bone Scaffold Engineering for Load Bearing Application. Handbook of Tissue Engineering. 2003.
[7] Hutmacher, DW. Scaffold in Tissue Engineering Bone and Cartilage. Biomaterial.s 2000; 21; 2529-43.

[8] De Muelder, ELW, Buma, P, Hanningk G. Anisotropic Porous Biodegradable Scaffolds for Muscoloskeletal Tissue Engineering; Materials. 2009; 2; 1674-96.
[9] Yun, HS, Kim, SH, Choi, J, Kim, HH, Kang, M. Biomimetic Component Coating on 3D Scaffolds using High Bioactivity of Mesoporous Bioactive Ceramics. Int. J. Nanomedicine. 2011; 6; 2521–31.

Acknowledgement
This research is funded by Ministry of Education and Cultural Republic of Indonesia in the year 2013.